CONF-921102--37

BEHAVIOR OF MIXED-OXIDE FUEL ELEMENTS DURING AN OVERPOWER TRANSIENT

H. Tsai and L. A. Neimark

Materials and Components Technology Division
ARGONNE NATIONAL LABORATORY
Argonne, Illinois 60439-4838 USA

ANL/MCT/CP--76422

DE93 004181

and

T. Asaga and S. Shikakura

Power Reactor and Nuclear Fuel Development Corporation (PNC)
Japan

NOVEMBER 1992

To be submitted to the 1992 Intl. Symposium on Reliable Fuels for Liquid Metal Reactors, November 15-20, 1992, Chicago, IL.

*Work supported by the U.S. Department of Energy, Office of Technology Support Programs, under Contract W-31-109-Eng-38.

Behavior of Mixed-Oxide Fuel Elements During an Overpower Transient*

by H. Tsai** , L. A. Neimark**, T. Asaga***, and S. Shikakura***

INTRODUCTION

For reliable operation of a fast breeder reactor, the fuel elements must be resistant to breaching in slow-ramp, operational overpower transients. To determine this resistance capability of mixed-oxide fuel elements, extended overpower transient tests over a range of element design and operating conditions are being conducted in the Experimental Breeder Reactor-II (EBR-II). These tests are a part of a collaborative Operational Reliability Testing (ORT) program between the U.S. Department of Energy and the Power Reactor and Nuclear Fuel Development Corp. (PNC) of Japan. The phase I portion of the program was successfully completed in 1990; the Phase II program is currently in progress.

Four extended overpower transient tests were conducted in the Phase-I ORT program. The results of the first three tests, TOPI-1A, -1B, and -1C, using existing preirradiated mixed-oxide fuel elements from the U.S. breeder development program, have been reported.[1,2] The results of the fourth test, TOPI-1D, using fuel elements specifically designed and fabricated for the ORT program, are the subject of this paper.

---

*Work supported by the U.S. Department of Energy, Office of Technology Support Programs, under Contract W-31-109-Eng-38.

**Materials & Components Technology Division, Argonne National Laboratory, Argonne, IL

***Power Reactor and Nuclear Fuel Development Corporation (PNC), Japan

1. TEST FUEL ELEMENTS AND VEHICLE

The TOPI-1D test consisted of nineteen preirradiated mixed-oxide fuel elements from the ORT TOP-4 subassemblies.[3,4] The elements had three types of cladding in two sizes: Type 316 and D9 with 5.84-mm OD and 0.38-mm wall, and D9 and PNC-316 with 6.99-mm OD and 0.37-mm wall. Both the D9 and PNC-316 materials are derivatives of Type 316 stainless steel with reduced void-swelling characteristics in fast neutron environments. All fuel elements had 343-mm-long fuel columns of solid $(U,Pu)O_2$ fuel pellets with dished ends, and a plenum-to-fuel volume ratio of ≈1.1-1.2. The range of pellet density was 85.3 - 94.6% TD, resulting in a fuel smeared density of 80.9 - 90.0% TD. The differences in fuel density, together with those in operating conditions, yielded fuel-element attributes that can be categorized as conservative, moderate and aggressive. A summary description of the fuel elements is given in Table 1.

Ten of the TOPI-1D test fuel elements were preirradiated under steady-state conditions and the remaining nine under steady-state plus duty-cycle (periodic 15% overpower transients) conditions. There were no discernible differences in the condition of the two groups of elements after the preirradiation [3], i.e., no apparent degradation due to the interspersed mild overpower transients. The preirradiation operating conditions for the TOPI-1D elements were generally aggressive: peak cladding inside surface temperatures of 600 - 670°C (life average) and peak linear powers of 30 TO 46 kW/m (at end of life). The element burnup range was 2.5 TO 9.7 at.%.

During the preirradiation in the TOP-4 subassemblies, each fuel element was contained in a double-wall, gas-gapped flow tube. [4] Individual orificing of the flow tubes allowed tailoring of the cladding temperature for every fuel element in the assemblies. The flow-tube assembly hardware also

had the advantage of permitting fuel elements of different diameters to be incorporated into the same assembly, as well as eliminating thermal and mechanical interactions between the fuel elements. For these reasons, the same type of assembly hardware was used in the TOPI-1D test.

2. TEST CONDUCT

The TOPI-1D test was conducted in a dedicated EBR-II run, 141C. To maximize the attainable fuel-element overpower in the transient, the TOPI-1D test assembly was placed at the center of the EBR-II core, which was specially configured to provide a spike of power density toward the core center. Furthermore, by increasing the reactor primary flow, the permissible peak reactor power was increased from 62.5 to 74 MWt. (The reactor power-to-flow ratio was maintained below unity throughout the transient.) With these provisions, the TOPI-1D test elements would reach their steady-state linear power ratings at a partial reactor power of ≈38.5 MWt.

Prior to the transient, the test fuel elements were preconditioned at this partial reactor power for seven days to re-establish the thermal and mechanical conditions that existed in the test fuel elements at the end of their last steady-state irradiation period. At the end of the preconditioning, without interruption, the reactor power was increased at a linear ramp of 0.1%/s from 38.5 to 73.3 MWt using the automatic control rod drive system. Immediately after reaching the peak power (at ≈910 s), the reactor was manually scrammed to terminate the transient. Figure 1 shows the reactor power history during the transient. The attained fuel element peak linear powers were 59 to 75 kW/m, corresponding to peak element overpowers of 64 to 99%, based on the element's linear power at the end-of-life (EOL). The cal-

culated power and cladding temperature histories for the fuel elements are summarized in Table 2.

Because the TOPI-1D test assembly had no built-in instrumentation, monitoring of fuel element breaching during the test relied on the EBR-II's two fuel element rupture detectors (FERDs) and a Ge-Li argon scanning system (GLASS) -- FERDs for detecting released delayed-neutron (DN) precursors in the primary coolant and GLASS for detecting released fission gases in the reactor plenum. Based on the GLASS data of ^{135}Xe ($t_{1/2}$ = 9.14 h) release, shown in Fig. 1, there was fuel element breaching during the TOPI-1D test. The initial breach occurred between 289 and 349 s, approximately one-third into the transient. The breach, however, did not cause any discernible DN release during or after the test. The longer-term fission-gas release histories for ^{135}Xe and ^{138}Xe ($t_{1/2}$ = 14.2 min) are shown in Fig. 2. It is significant to note that the release of the shorter half-life ^{138}Xe gas did not occur until after the reactor scram, suggesting the release was associated with the cracking of the fuel during shutdown. Both the GLASS and FERD data shown in Figs. 1 and 2 have been corrected for their respective transport delays.

3. TEST RESULTS

3.1 Breach Determination

Using visual inspection, element weighing, and plenum gamma (^{133}Xe) scanning techniques, WT129, a small-diameter (5.84 mm) element with 316SS cladding and a moderate design, was identified to be the only breached element in the TOPI-1D test. At the time of breach, the overpower of the element was 22 to 27%, based on its EOL element linear power. The weight loss of the element was minimal and could be accounted for with a loss of ≈40% of

the fission gas inventory. The breach was a narrow longitudinal crack ≈5.0-mm long at an axial location of X/L = 0.86 directly under the wrapping wire.

The WT129 element had a brief overtemperature operating history during its initial steady-state irradiation in EBR-II Run 128. The overtemperature was apparently the result of an improper element wire-wrap pitch (305 mm), which allowed element bowing to cause cladding/flow tube contact. After the problem was identified, the wire pitch for WT129 was modified (to 97 mm) and irradiation was continued. Although WT129 survived its irradiation to 9.7 at.%, the operation in Run 128 apparently caused irreversible damage to the cladding as evidenced by a large (1.7% max) and axially-nonuniform cladding strain before the transient. For these reasons, the breach of this element was judged to be anomalous for the purpose of this test. However, even for this flawed element, breaching occurred at an overpower approximately twice the trip settings of reactor plant protection systems (≈10-12% overpower). Moreover, the behavior of the breach was benign, i.e., it resulted in no apparent release of fuel.

All other elements in the TOPI-1D test, including the other five that also experienced similar overtemperature in Run 128, maintained their cladding integrity. A very substantial cladding integrity margin was thus demonstrated. The duty-cycle transients imposed on nine of the test elements in the preirradiation apparently had negligible effects on the cladding integrity margin.

3.2 Fuel Column Elongation

Approximately half the fuel elements in the TOPI-1D test incurred an elongation of the fuel column, based on the comparison of the pre- and posttest neutron radiographic and gamma scanning data. The results are sum-

marized in Table 3. The maximum elongation was 3.6% in element WT187. In general, the greatest elongation occurred in fuel elements with the greatest transient linear power. All of the measurable elongation took place at the top end of the fuel column, in the form of either transverse fuel pellet cracking or lifting of the fuel top by molten fuel. These features are illustrated in Fig. 3, which shows the radiographs of elements WT171 (1.1% dL/L, transverse pellet cracking) and WT187 (3.6% dL/L, molten fuel liftoff). The formation of an enlarged, irregular, or discontinuous central void as seen in the neutron radiographs is evidence of fuel melting and motion.

3.3 Cladding Deformation

The cladding diameter profiles for the test elements were measured with laser profilometry before and after the transient. The scans were performed in linear paths at 9° azimuthal intervals with the wire wrap removed. Results from the multi-angle scans were averaged to yield the cladding diameter at a given elevation over the length of the fuel element.

Transient-induced cladding strains for the TOPI-1D fuel elements ranged from <0.1% for conservative elements, 0.06 - 0.32% for moderate elements, and 0.05 to 1.50% for aggressive elements. The data are summarized in Table 3. To illustrate the performance differences of the D9 and PNC-316 cladding materials, the cladding diameter and strain profiles of elements WT182 (D9-clad) and WT171 (PNC-316-clad) are compared in Figs. 4 and 5. The two elements had the same aggressive design features and operated under comparable preirradiation and transient conditions (see Tables 1 and 2). The PNC-316 cladding material appeared to have a superior strain behavior to the D9 cladding during steady-state operation; the transient behavior of the ma-

terials, however, was comparable. Within a group of large-diameter, aggressive D9- and PNC-316-clad elements, the transient-induced strain is a strong function of the overpower, as shown in Fig. 6.

The data on cladding strain and fuel column elongation (Table 3) suggest that there is a tradeoff between the two phenomena, i.e., if fuel column is allowed to grow upward, the radial strain of the cladding would be reduced. An example is the comparison between elements WT179 (2.9% fuel elongation and 0.70% transient strain) and WT180 (0.0% fuel elongation and 1.5% transient strain.)

3.4 Fission-gas Release

Fission-gas release was measured for five elements: WT171, WT180 and WT183 with ≈7 at.% burnup, and WT036R and WT187 with ≈3 at.% burnup. The respective results were 96, 95 and 85% for the three higher burnup elements and 86 and 71% for the two lower burnup elements. A comparison with steady-state sibling data [5] indicates little additional fission-gas release during the transient for the higher burnup elements. For the lower burnup elements, however, there appears to be a notable incremental release (≈10 to 20%) during the transient.

3.5 Fuel and Cladding Microstructures

Centerline fuel melting occurred in all test elements during the transient, as evidenced on the posttest neutron radiographs. This was confirmed metallographically in all five elements destructively examined. Figure 7 shows the transverse midplane section of element WT036R, which had D9 cladding, low fuel smear density (81.1% TD), low burnup (3.4 at.%), and high transient power (79.8 kW/m). Centerline fuel melting was extensive (≈50%

areal melt fraction), owing to the low smear-density, hence low conductivity, fuel. Melting apparently extended partly into the gaseous, equiaxed-grain-growth region, contributing to the aforementioned transient fission-gas release. At the top of the WT036R element, shown in Fig. 8, the molten fuel lifted the top insulator pellet and filled the resultant void space. Molten fuel resolidified on the cladding inside surface and caused limited cladding melting (Fig. 9). The driving force for the upward movement of the molten fuel was evidently the fission-gas pressure in the central cavity.

The microstructure of the midplane section of a higher burnup (7.1 at.%) element WT179, with PNC-316 cladding, high fuel smear density (89.7% TD), and high transient power (74.4 kW/m), is shown in Fig. 10. Attributable to the higher fuel density, centerline melting was less extensive (≈32% areal) and did not extend beyond the columnar-grain region. Plutonium migration to the fuel periphery and cesium migration to the fuel periphery and fuel/cladding interface is evident on the alpha and beta-gamma autoradiographs (Fig. 10). Further evidence of cesium migration was the dark, loose appearance of the fuel periphery. Intergranular cladding penetration due to fuel/cladding chemical interaction, to a depth of 25 μm, is shown in Fig. 11. The longitudinal section at the top of the WT179 fuel column, Fig. 12, shows the UO_2 insulator pellets were raised ≈9 mm with molten fuel up around the bottom insulator pellet. Fission-gas in the central cavity could account for the upward molten fuel movement. Fragments of the top of the fuel column were present in the molten fuel.

4. CONCLUSIONS

The TOPI-1D extended overpower transient test demonstrated that conservative, moderate and aggressive design mixed-oxide fuel elements at 2.5 to 9.7 at.% burnup can survive a 65-99% transient overpower event at a low ramp rate of 0.1%/s. The breach of element WT129 was deemed anomalous due to its preirradiation history which included a brief period of substantial overheating early in life. The TOPI-1D results, coupled with the data from the prior transient tests (TOPI-1A, -1B, and -1C) provide a comprehensive transient data base on first-generation (high-swelling Type 316 stainless steel) and second-generation (low-swelling D9 and PNC 316) cladding materials. This data base can be used for development, calibration, and validation of fuel performance computer codes, e.g., PNC's CEDAR.

The measured peak transient-induced cladding diametral strain for the aggressive design fuel elements with D9 and PNC-316 cladding ranged from 0.21 to 1.5%. The magnitude of the transient-induced strain was independent of the prior steady-state strain and generally increased with increasing levels of transient overpower and fuel smear density.

Extensive fuel melting occurred in all elements during the overpower transient. Areal melting ranged from approximately 20 to 50% with peak transient linear powers of 74 to 80 kW/m. Significantly, melting did not cause any of the fuel elements to breach, although it had a strong impact on the other aspects of fuel element behavior. As the gas pressure in the central cavity increased during the transient due to the increased centerline temperature and melting-induced fission gas release, it exerted stresses in both the radial and axial directions. The former contributed to cladding strain (in 17 out of 19 elements, ranging from 0.1 to 1.5%) and the latter caused the lifting of the top of the fuel column (in eight elements, ranging

from 0.1 to 3.6% DL/L). The effect of axial fuel motion was a relief of the center cavity pressure and hence the stress on the cladding. It is significant to note that, of the 19 elements, the highest cladding strain (1.5%) occurred in an element which incurred no fuel axial expansion.

5. REFERENCES

[1] H. Tsai, et al., "Extended Overpower Transient Testing of LMFBR Oxide Pins in EBR-II," Proceedings of the Conference on Nuclear Fuel Performance in Stratford-upon-Avon, Vol. 1, pp. 287-293, March 25-29, 1985.

[2] H. Tsai, et al., "Performance of Fast Reactor Mixed-oxide Fuel Pins during Extended Overpower Transients," Trans. of the 11th International Conference on Structural Mechanics in Reactor Technology, Vol. C, pp. 179-184, August 18-23, 1991.

[3] A. Boltax, et al., "Fuel Pin Behavior during Duty Cycle Testing," Proceedings of the 1990 International Fast Reactor Safety Meeting, Vol. IV, pp. 155-164, Snowbird UT, August 12-16, 1990.

[4] P. J. Levine, et al., "EBR-II Duty Cycle Testing of Fuel and Blanket Rods," Proceedings of International Conference on Reliable Fuels for Liquid Metal Reactors, pp. 6.35-6.47, Tucson AZ., September 7-11, 1986.

[5] A. Boltax, et al., "Reliability of Fast Reactor Mixed-Oxide Fuel During Operational Transients," Proceedings of the International Conference on Fast Reactors and Related Fuel Cycles, Vol. I, pp. 6.6-1-11, Kyoto, October 28-November 1, 1991.

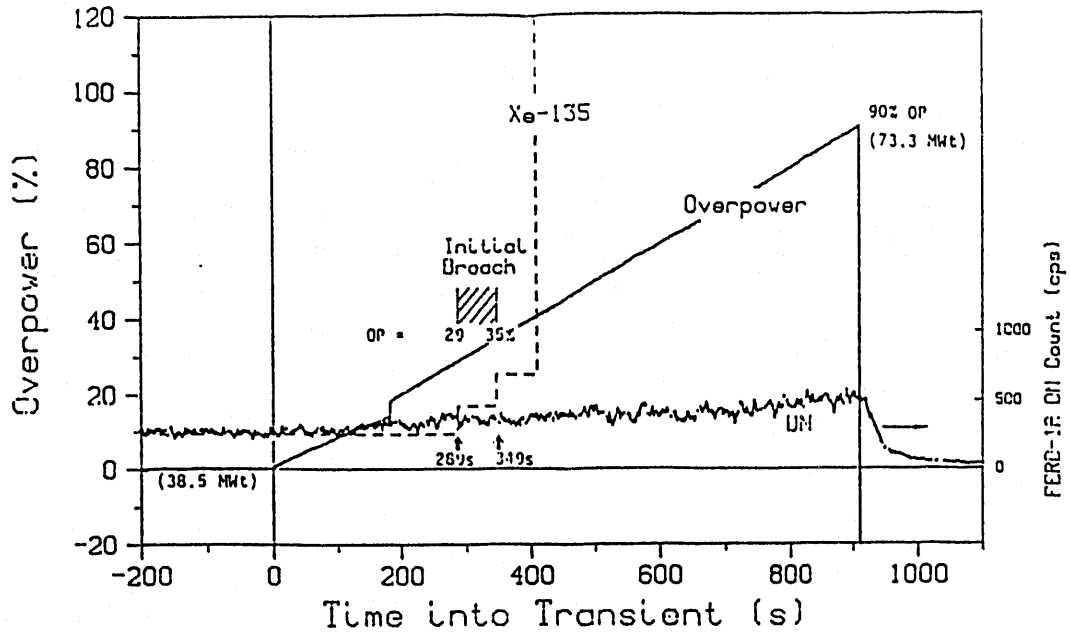

Fig. 1. Summary of the TOPI-1D Test Operations.

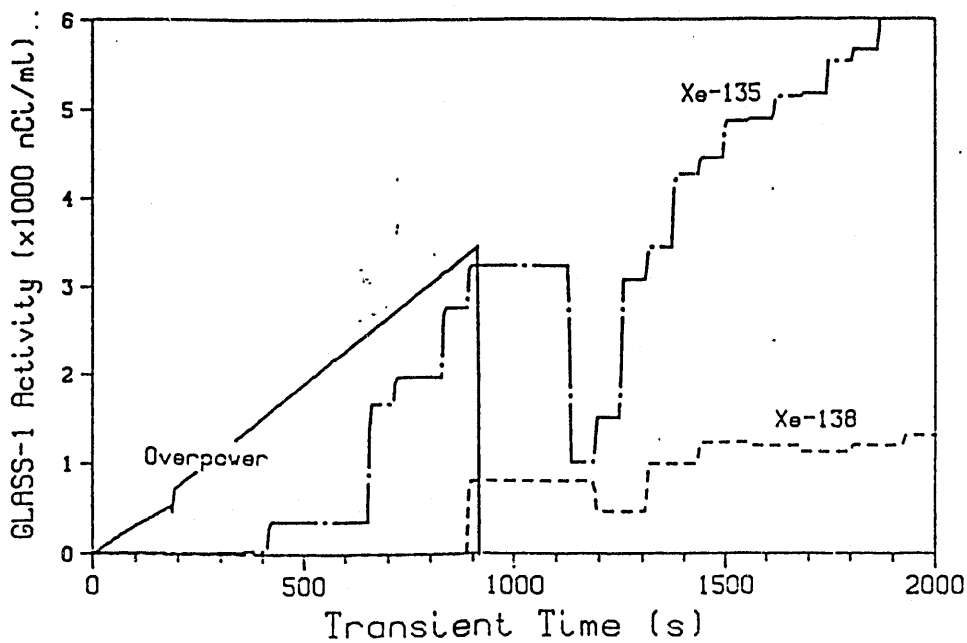

Fig. 2. Fission-Gas Release during the TOPI-1D Test.

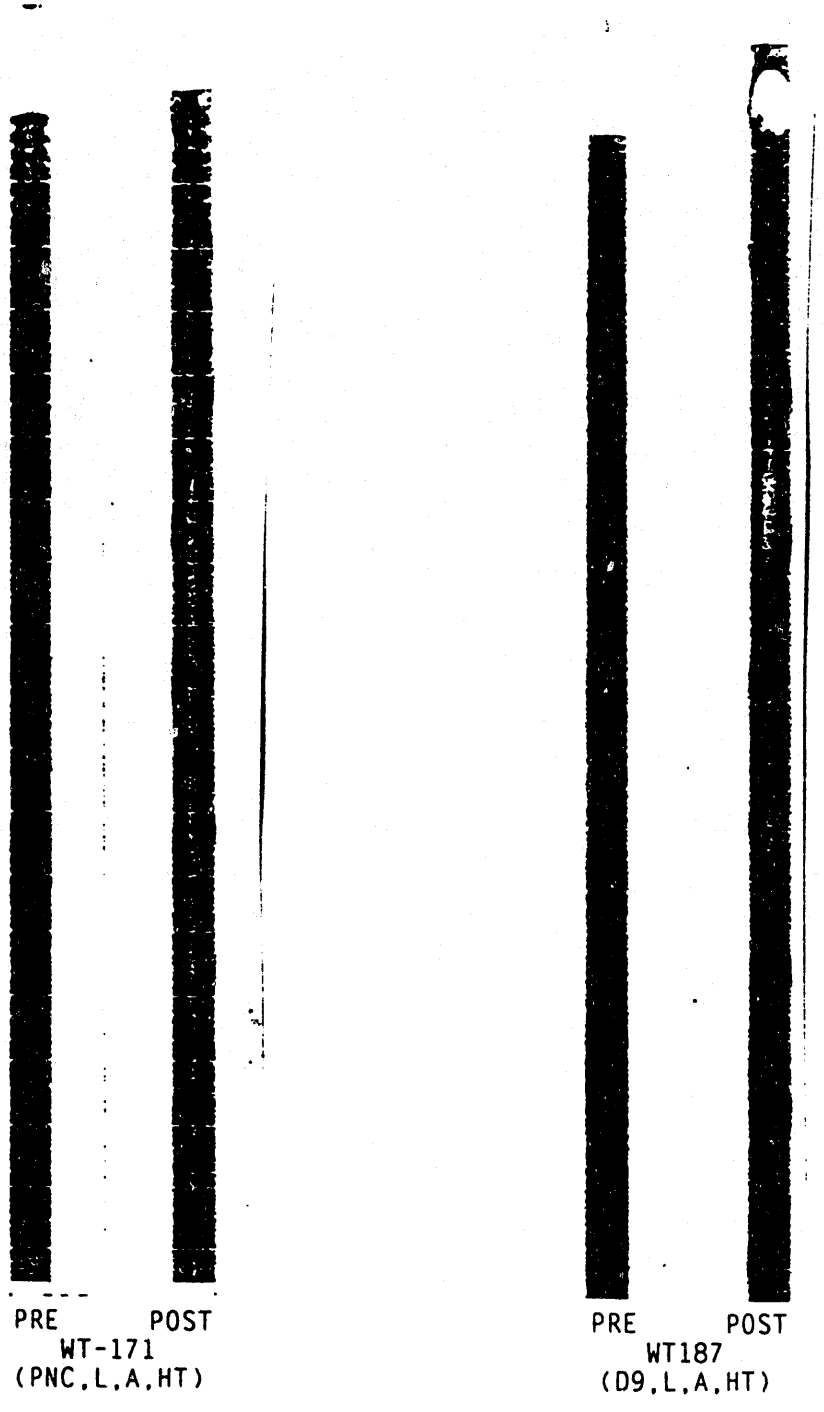

Fig. 3. Pre- and Posttransient Neutron Radiographs of TOPI-1D Elements WT171 and WT187 between X/L = 0.5 and 1.

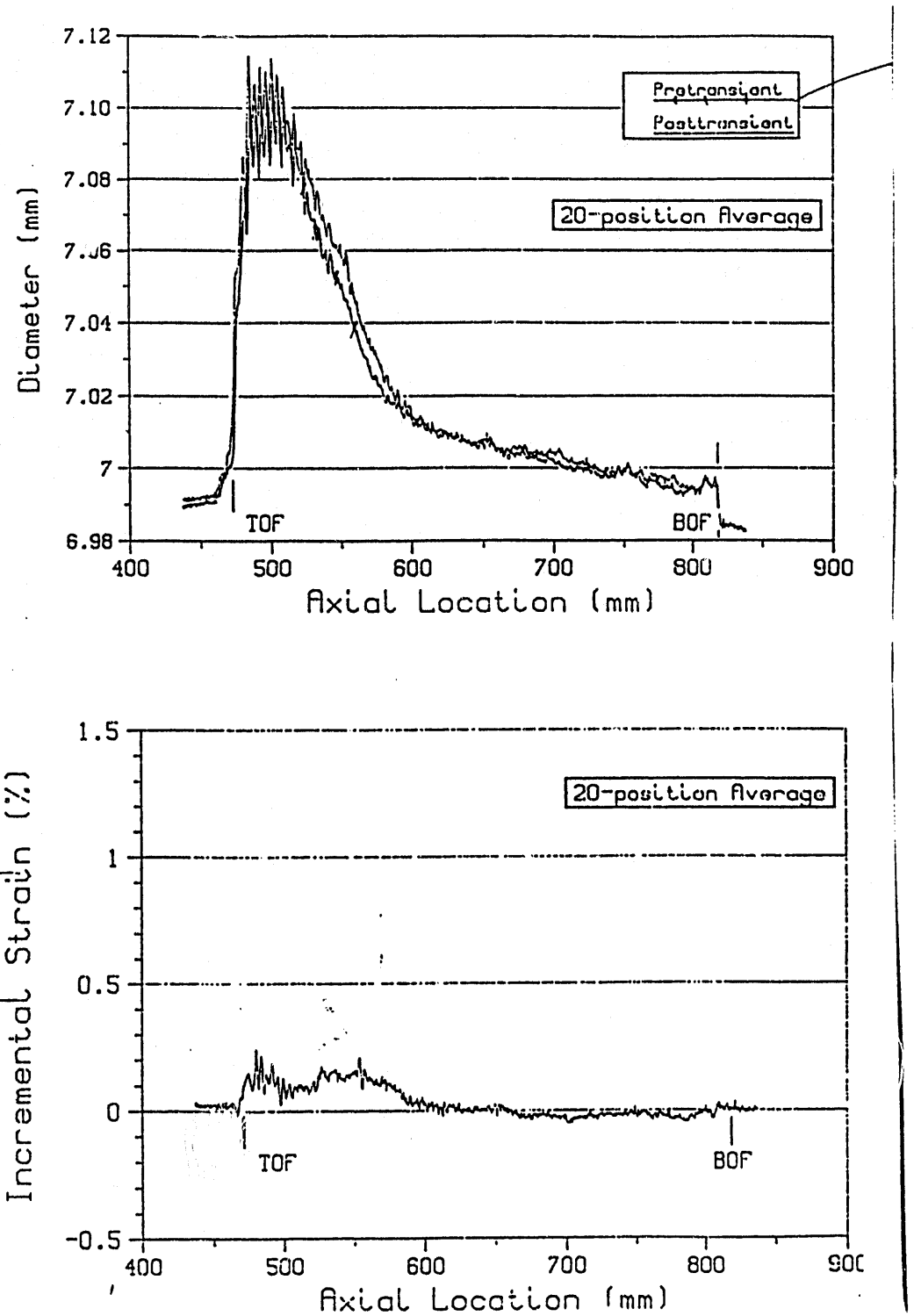

Fig. 4. Cladding Diameter and Incremental Strain Profiles for TOPI-1D Element WT182 (D9,L,A,HT).

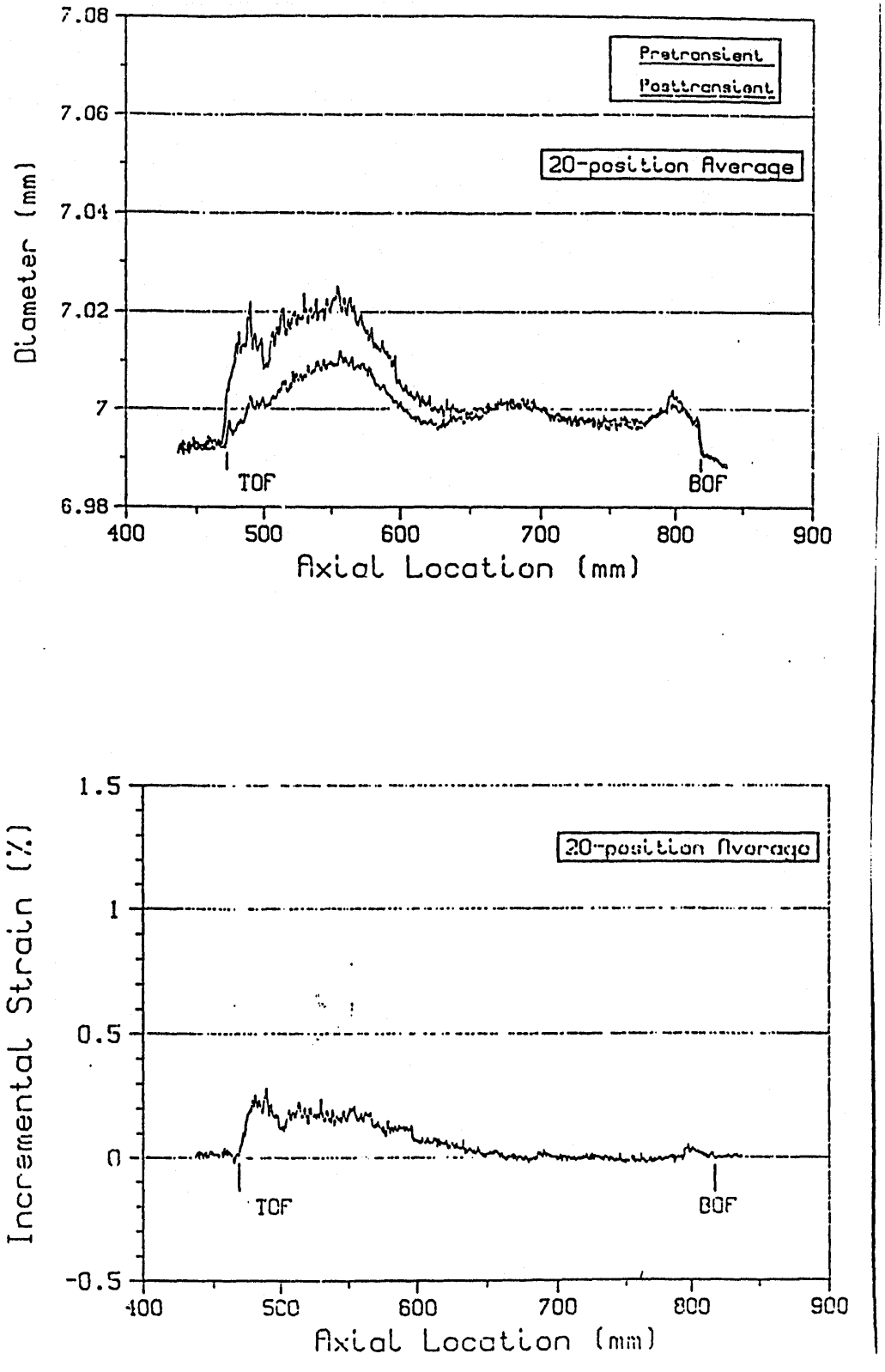

Fig. 5 Cladding Diameter and Incremental Strain Profiles for TOPI-1D Element WT171 (PNC,L,A,HT).

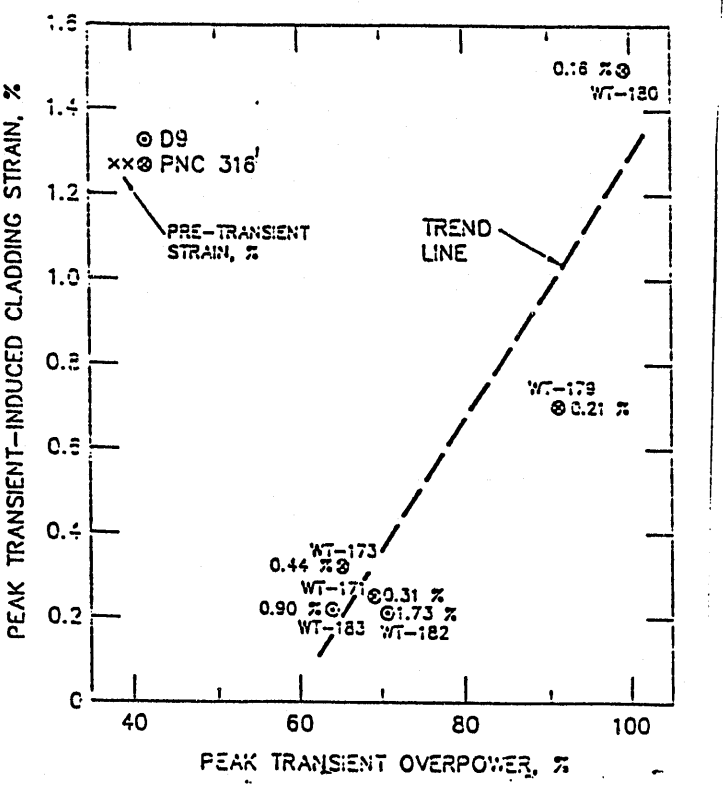

Fig. 6. Dependence of Transient Cladding Strain on Element Overpower for a Group of Aggressive, Large-diameter Elements.

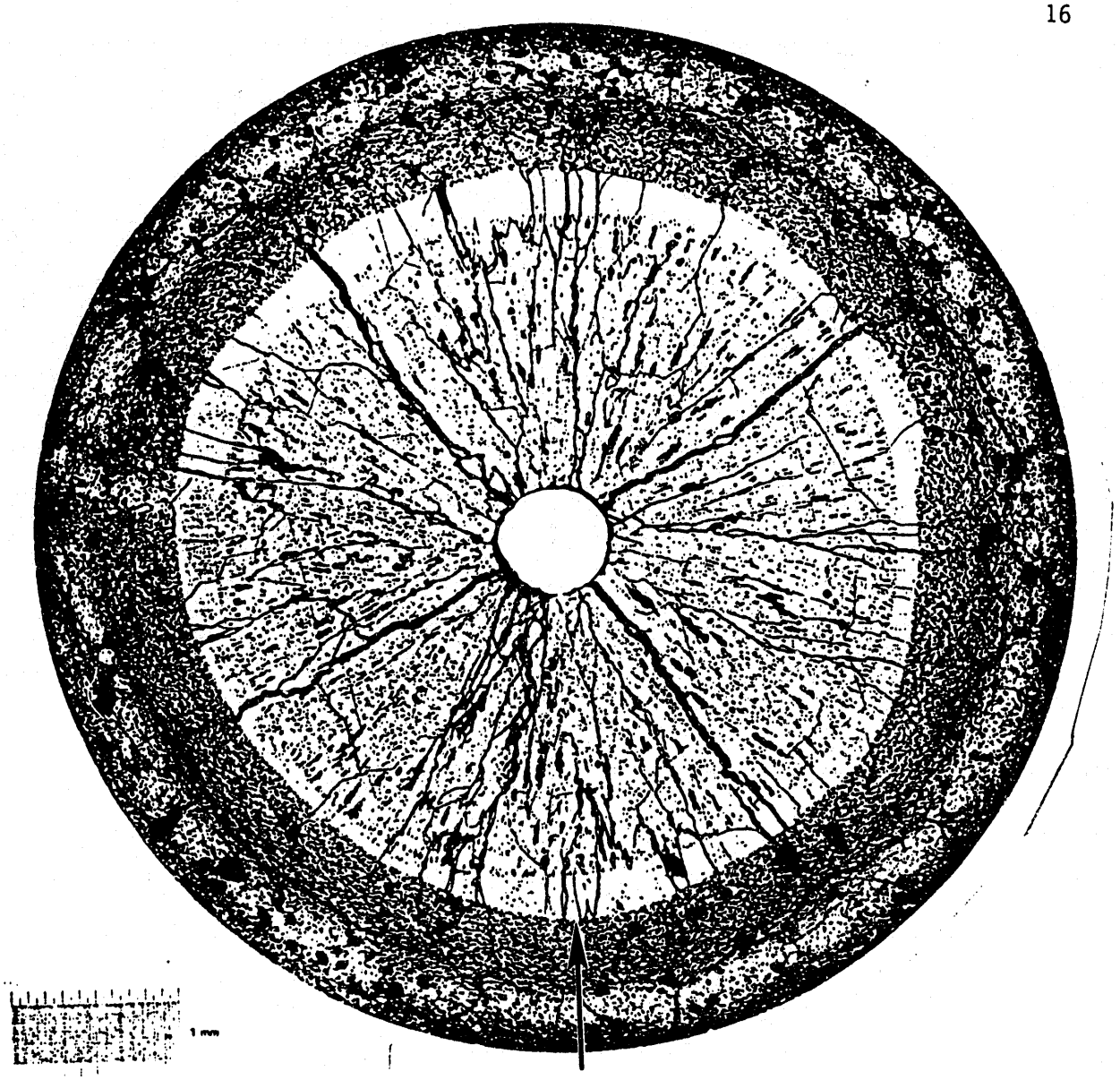

Fig. 7. Transverse Photomicrograph of Element WT036R at the Axial Midplane. Arrow denotes the boundary of fuel melting. The bright particle at the center is a metallic fission-product ingot.

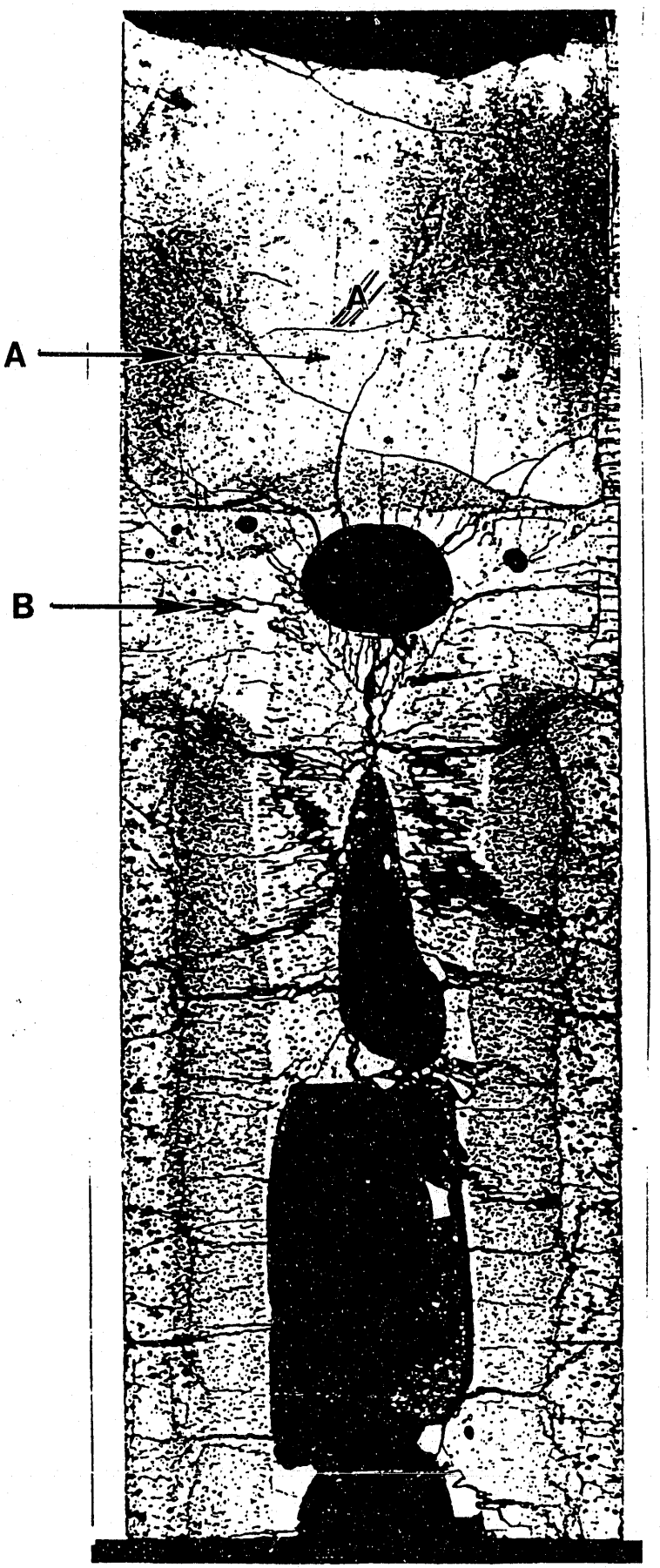

Fig. .8

Longitudinal Section of Element WT036R at the Fuel Top Showing the Lifting of the UO_2 Insulator Pellet (A) by Molten Fuel (B).

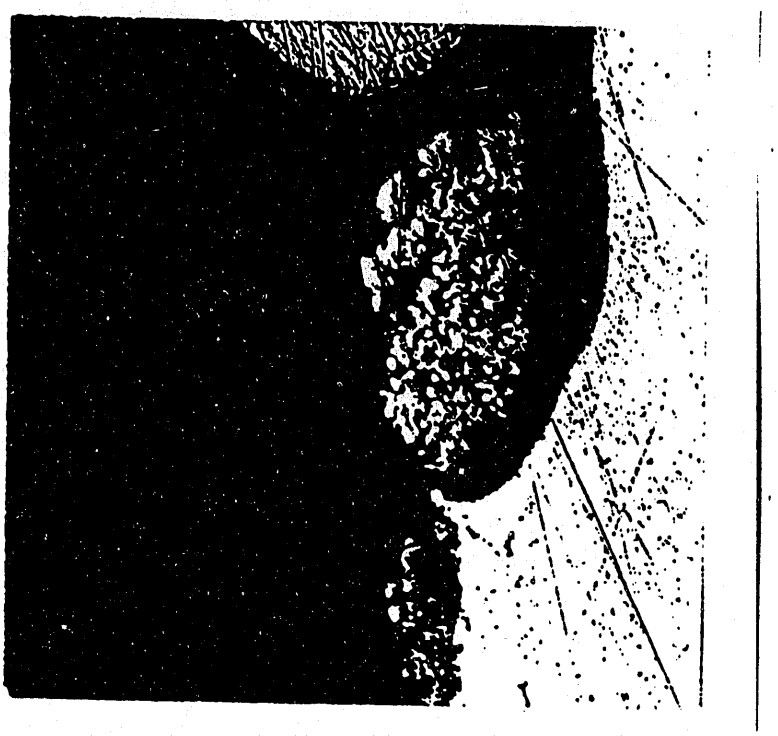

Fig. 9. Cladding Melting due to the Molten Fuel in Element WT036R at X/L = 1.0 (as polished, 750X).

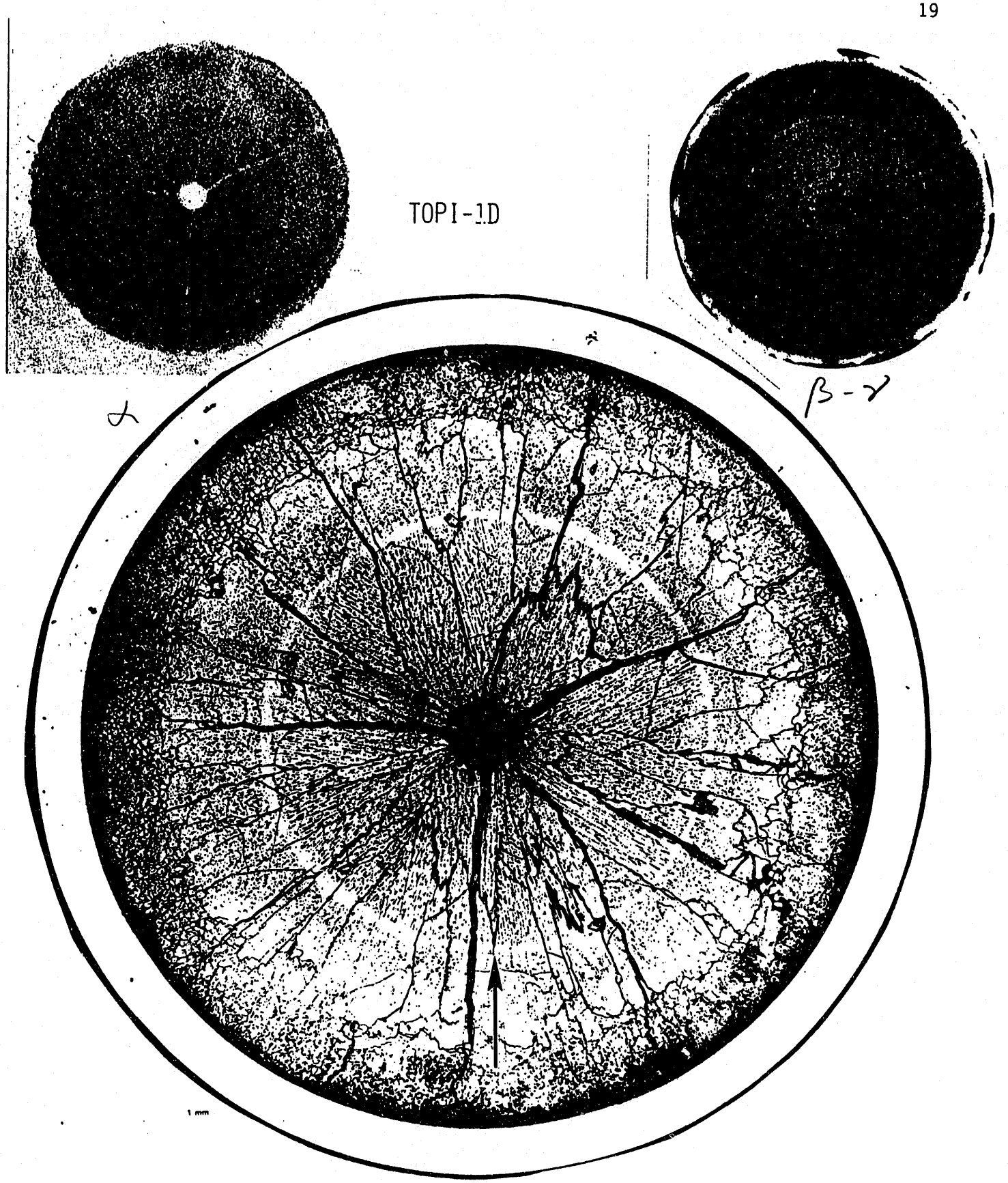

Fig. 10. Transverse Section of Element WT179 at the Axial Midplane. Arrow denotes the radial extent of fuel centerline melting.

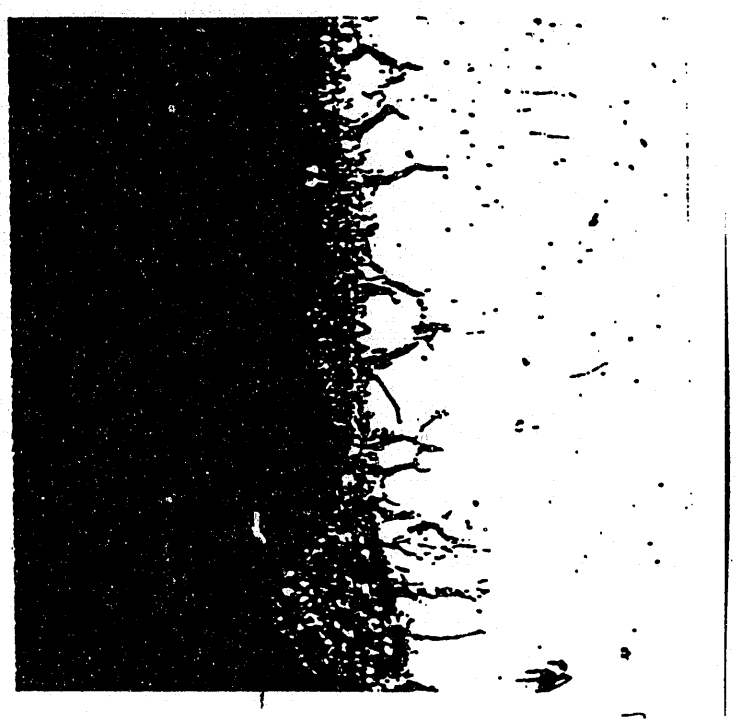

Fig. 11. Intergranular Cladding Penetration in Element WT179.

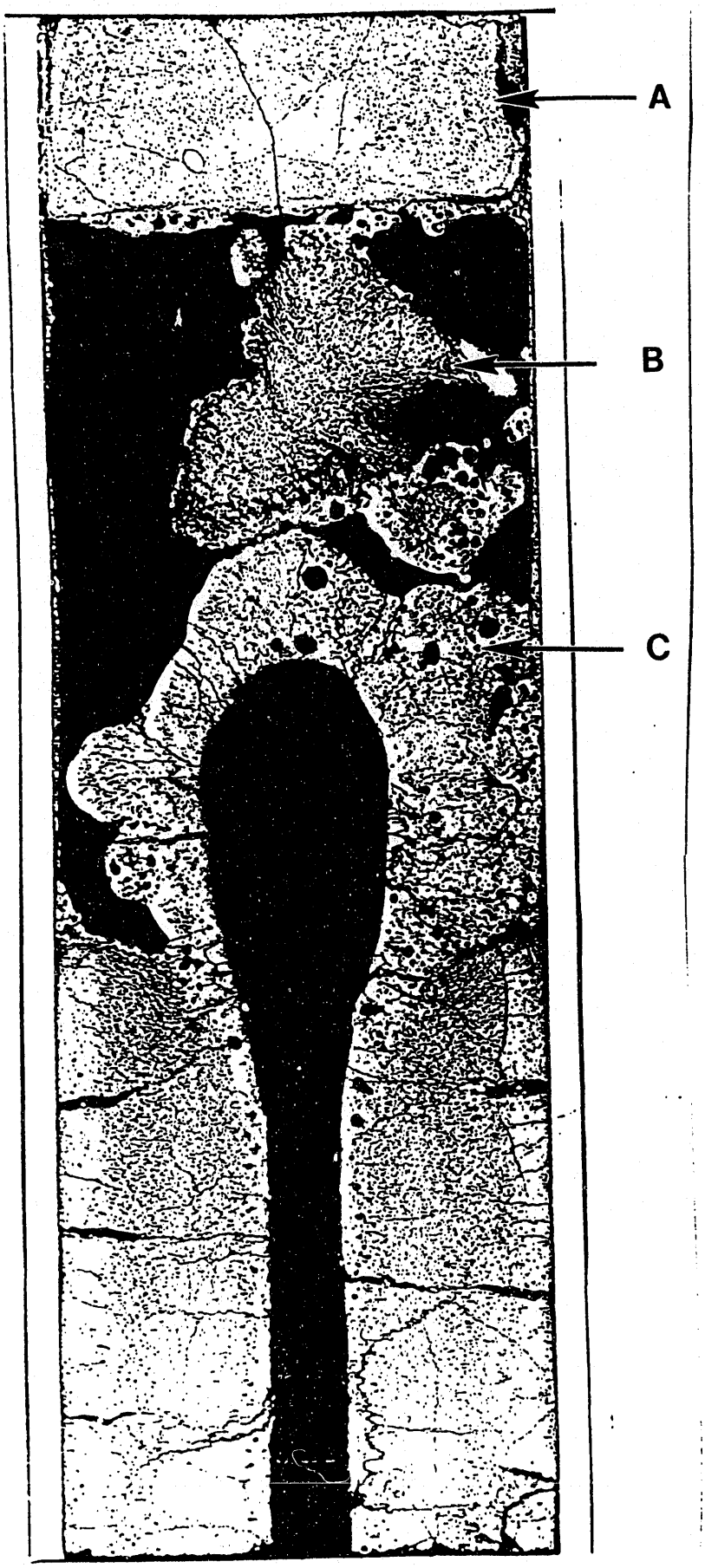

Fig. .12

Longitudinal Section of Element WT179 at the Top of Fuel. A: raised UO_2 insulator pellet; B: remnant of the previous fuel top; C: once-molten fuel.

Table 1. Summary Description of the TOPI-1D Test Elements

Test Element	Element Type[1]	Source S/A	Run 128[2]	Time-Averaged Clad ID Temp.(°C)	EOL Power (kW/m)	Peak BU (at.%)	Peak Fast Fluence 10^{22}n/cm^2	Clad[3] OD (mm)	Pellet Density (% TD)	Pellet Diam. (mm)	Diam. Gap (mm)	Smear Density (% TD)	Fuel O/M	Pu Content (wt.%)	^{235}U Enrich. (%)	Plenum /Fuel Ratio
WT127	316,S,M,LT	TOP-4A	No	615	35.9	8.5	6.0	5.842	93.4	4.996	0.084	90.3	1.96	33.0	89	1.18
WT171	PNC,L,A,HT	TOP-4A	No	650	44.3	6.8	5.9	6.985	94.6	6.162	0.086	89.7	1.97	22.5	66	1.12
WT182	D9,L,A,HT	TOP-4A	No	650	43.9	6.8	5.9	6.985	94.6	6.162	0.086	89.7	1.97	22.5	66	1.12
WT183	D9,L,A,HT	TOP-4A	No	655	45.6	7.1	6.1	6.985	94.6	6.162	0.086	89.7	1.97	22.5	66	1.12
WT011	D9,L,C,LT	TOP-4AA	4A	610	34.6	6.4	6.9	6.985	90.3	6.093	0.155	85.9	1.95	22.5	45	1.12
WT107	D9,L,M,HT	TOP-4AA	4AA	640	42.4	7.7	6.8	6.985	92.9	6.149	0.099	90.0	1.97	22.5	66	1.12
WT108	D9,L,M,HT	TOP-4AA	4AA	640	43.5	7.9	6.9	6.985	92.9	6.149	0.099	90.0	1.97	22.5	66	1.12
WT118	D9,S,M,HT	TOP-4AA	No	650	34.7	9.3	6.6	5.842	93.4	4.996	0.084	90.3	1.96	33.0	89	1.18
WT129	316,S,M,HT	TOP-4AA	4AA	640	34.7	9.7	6.8	5.842	93.4	4.996	0.084	90.3	1.96	33.0	89	1.18
WT173	PNC,L,A,HT	TOP-4AA	No	665	44.3	7.8	6.9	6.985	94.6	6.162	0.086	89.7	1.97	22.5	66	1.12
WT028	D9,L,M,LT	TOP-4B	No	630	35.0	2.5	2.6	6.985	90.4	6.165	0.084	88.0	1.95	22.5	45	1.12
WT036R	D9,L,A,HT	TOP-4B	No	670	43.7	3.4	2.6	6.985	85.3	6.096	0.152	81.1	1.99	33.0	75	1.12
WT187	D9,L,A,HT	TOP-4B	No	655	45.4	3.2	2.7	6.985	94.6	6.162	0.086	89.7	1.97	22.5	66	1.12
WT008	PNC,L,C,LT	TOP-4BB	4BB	625	30.2	6.2	6.3	6.985	84.5	6.114	0.135	80.9	1.99	30.0	45	1.12
WT022	D9,L,C,LT	TOP-4BB	4BB	600	31.8	6.0	6.5	6.985	90.3	6.093	0.155	85.9	1.95	30.0	45	1.12
WT033	D9,L,M,LT	TOP-4BB	No	600	33.1	5.9	6.4	6.985	90.4	6.165	0.084	88.0	1.95	30.0	45	1.12
WT136	316,S,M,HT	TOP-4BB	No	640	32.5	8.9	6.2	5.842	93.4	4.996	0.084	90.3	1.96	33.0	89	1.18
WT179	PNC,L,A,HT	TOP-4BB	No	650	39.0	7.1	6.2	6.985	94.6	6.162	0.086	89.7	1.97	22.5	66	1.12
WT180	PNC,L,A,HT	TOP-4BB	No	635	37.6	6.9	6.1	6.985	94.6	6.162	0.086	89.7	1.97	22.5	66	1.12

[1] D9, 316, PNC: Denote the three types of cladding materials.
L, S: Denote Large (≈7.0-mm)- or Small (≈5.8-mm)-diameter cladding.
C, M, A: Denote Conservative, Moderate, or Aggressive element design.
HT, LT: Denote High or Low cladding temperature, where the dividing temperature is 630°.

[2] Elements in Run 128 experienced brief overtemperature operation. See text.

[3] Cladding thickness for all elements was 0.37-0.38 mm.

Table 2. Irradiation Conditions of the TOPI-1D Test Elements

Element	Element Type	BU (at.%)	Steady-State EOL Power LHR (kW/m)	Steady-State BU-Avg. PCIT (°C)[1]	Preconditioning Power (kW/m)	Preconditioning PCIT (°C)	Transient Peak Power (kW/m)	Transient Peak PCIT (°C)	Transient Peak Overpower[2] (%)
WT127	316,S,M,LT	8.5	35.9	615	31.7	627	60.4	857	68
WT171	PNC,L,A,HT	6.8	44.3	650	39.3	620	74.9	847	69
WT182	D9,L,A,HT	6.8	43.9	650	39.3	624	74.9	853	71
WT183	D9,L,A,HT	7.1	45.6	655	39.2	619	74.6	844	64
WT011	D9,L,C,LT	6.4	34.6	610	30.7	625	58.5	856	69
WT107	D9,L,M,HT	7.7	42.4	640	38.8	617	73.9	841	74
WT108	D9,L,M,HT	7.9	43.5	640	38.5	619	73.3	844	68
WT118	D9,S,M,HT	9.3	34.7	650	31.7	641	60.3	885	74
WT129	316,S,M,HT	9.7	34.7	640	31.2	637	59.4	877	71
WT173	PNC,L,A,HT	7.8	44.3	665	38.5	604	73.3	815	65
WT028	D9,L,M,LT	2.5	35.0	630	33.6	577	63.9	766	82
WT036R	D9,L,A,HT	3.4	43.7	670	41.9	629	79.8	862	83
WT187	D9,L,A,HT	3.2	45.4	655	41.7	627	79.3	858	75
WT008	PNC,L,C,LT	6.2	30.2	625	31.3	628	59.5	862	97
WT022	D9,L,C,LT	6.0	31.8	600	30.8	594	58.7	797	84
WT033	D9,L,M,LT	5.9	33.1	600	31.6	574	60.1	759	82
WT136	316,S,M,HT	8.9	32.5	640	31.8	642	60.6	887	86
WT179	PNC,L,A,HT	7.1	39.0	650	39.1	622	74.4	850	91
WT180	PNC,L,A,HT	6.9	37.6	635	39.4	624	75.0	853	99

[1]PCIT = Peak cladding inside surface temperature.

[2]Overpower (%) = {Transient LHR/EOL LHR) - 1} 100. The percentage overpower referenced to the preconditioning period was 90% for all pins.

Table 3. TOPI-1D Cladding Diametral Strain and Fuel Column Elongation

Element	Transient Strain		Fuel Column Elongation, %
	%	Location (X/L)	
WT127	0.20	0.9, 1.0	0.0
WT171	0.27	1.0	1.1
WT182	0.21	1.0	1.4
WT183	0.33	1.0	1.5
WT011	0.07	0.7	0.0
WT107	0.10	0.6, 1.0	0.0
WT108	0.12	1.0	0.5
WT118	0.25	0.9, 1.0	0.0
WT129	0.32	0.9	0.0
WT173	0.32	0.9	2.6
WT028	0.15	0.8	0.1
WT036R	0.05	0.9	0.7
WT187	0.10	0.5, 0.9	3.6
WT008	0.00	-	0.0
WT022	0.00	-	0.0
WT033	0.06	0.9	0.0
WT136	0.10	1.0	0.0
WT179	0.70	1.0	2.9
WT180	1.50	0.9, 1.0	0.0

END

DATE
FILMED
2/19/93